JOURNAL OF GEOPHYSICAL RESEARCH, VOL. 108, NO. D8, 8441, doi:10.1029/2002JD002650, 2003

PMSE dependence on aerosol charge number density and aerosol size

Markus Rapp, Franz-Josef Lübken, Peter Hoffmann, Ralph Latteck, and Gerd Baumgarten
Leibniz-Institute of Atmospheric Physics, Kühlungsborn, Germany

Tom A. Blix
Norwegian Defence Research Establishment, Kjeller, Norway

Received 13 June 2002; revised 24 July 2002; accepted 25 July 2002; published 11 February 2003.

[1] It is commonly accepted that the existence of polar mesosphere summer echoes (PMSEs) depends on the presence of charged aerosols since these are comparatively heavy and reduce the diffusion of free electrons due to ambipolar forces. Simple microphysical modeling suggests that this diffusivity reduction is proportional to r_A^2 (r_A = aerosol radius) but only if a significant amount of charges is bound on the aerosols such that $N_A|Z_A|/n_e > 1.2$ (N_A = number of aerosols, Z_A = aerosol charge, n_e = number of free electrons). The fact that the background electron profile frequently shows large depletions (“biteouts”) at PMSE altitudes is taken as a support for this idea since within biteouts a major fraction of free electrons is missing, i.e., bound on aerosols. In this paper, we show from in situ measurements of electron densities and from radar and lidar observations that PMSEs can also exist in regions where only a minor fraction of free electrons is bound on aerosols, i.e., with no biteout and with $N_A|Z_A|/n_e \ll 1$. We show strong experimental evidence that it is instead the product $N_A|Z_A|r_A^2$ that is crucial for the existence of PMSEs. For example, small aerosol charge can be compensated by large aerosol radius. We show that this product replicates the main features of PMSEs, in particular the mean altitude distribution and the altitude of PMSEs in the presence of noctilucent clouds (NLCs). We therefore take this product as a “proxy” for PMSE. The agreement between this proxy and the main characteristics of PMSEs implies that simple microphysical models do not satisfactorily describe PMSE physics and need to be improved. The proxy can easily be used in models of the upper atmosphere to better understand seasonal and geographical variations of PMSEs, for example, the long debated difference between Northern and Southern hemisphere PMSEs. *INDEX TERMS:* 0305 Atmospheric Composition and Structure: Aerosols and particles (0345, 4801); 0340 Atmospheric Composition and Structure: Middle atmosphere—composition and chemistry; 2439 Ionosphere: Ionospheric irregularities; 6929 Radio Science: Ionospheric physics (2409)

Citation: Rapp, M., F.-J. Lübken, P. Hoffmann, R. Latteck, G. Baumgarten, and T. A. Blix, PMSE dependence on aerosol charge number density and aerosol size, *J. Geophys. Res.*, *108*(D8), 8441, doi:10.1029/2002JD002650, 2003.

1. Introduction

[2] Polar mesosphere summer echoes (PMSEs) are intriguingly strong radar echoes which were first observed in the VHF band in the late 1970s [*Czechowsky et al.*, 1979; *Ecklund and Balsley*, 1981]. Coherent radar echoes from the mesosphere require electron number density fluctuations at the Bragg scale (=radar half wavelength), which is 3 m for a 50-MHz radar [*Tatarskii*, 1971]. First ideas that the echoes were due to pure neutral air turbulence were soon disregarded since energy dissipation rates of ∼100 W/kg were needed whereas observational evidence showed that typical values were rather on the order of 0.1 W/kg (for an overview of the observational database, see *Lübken* [1997]). This, however, means that the radar Bragg scale for VHF radars is far in the viscous subrange of turbulence such that irregularities at these scales should be efficiently smoothed out by molecular diffusion. A first breakthrough was achieved through the work of *Kelley et al.* [1987] and *Cho et al.* [1992], who argued that large positive ion clusters or charged aerosol particles could efficiently slow down the diffusion of electrons by ambipolar forces. This picture was substantially corroborated by in situ results of electron number density measurements which showed deep depletions at PMSE altitudes [e.g., *Ulwick et al.*, 1988]. These “biteouts” occur because of electron attachment to aerosol particles [e.g., *Reid*, 1990] which are known to exist in close vicinity to PMSEs from simultaneous observations of noctilucent clouds (NLCs) and PMSEs [*von Zahn and Bremer*, 1999]. In a strong biteout situation the majority of negative charge resides on negatively charged aerosol particles which then reduce the electron mobility due to ambipolar forces.

[3] Based on these results, the necessary conditions for the existence of PMSE (=the existence of electron fluctuations at the Bragg scale) can be summarized as follows:

0148-0227/03/2002JD002650$09.00

first, there must be an excitation mechanism which creates irregularities in the electron gas initially. Second, there must be a sufficient amount of charged aerosol particles, which efficiently reduce electron mobility such that, once created, small-scale electron fluctuations can prevail at scales of the radar half wavelength.

[4] As far as the excitation mechanism is concerned the most common assumption has been that it is isotropic neutral air turbulence which initially creates irregularities in the electron gas [e.g., *Klostermeyer*, 1997; *Hill et al.*, 1999]. However, there is now firm experimental evidence that neutral air turbulence is of minor if not negligible importance [*Lübken et al.*, 1993, 2002]. Alternative theories have been proposed (for a discussion, see *Cho and Röttger* [1997] and *Blix* [1999]) but firm conclusions have not yet been presented so that the question for the excitation mechanism must be considered unanswered.

[5] The main objective of the current paper is a refinement of our understanding of the role of charged aerosol particles for the existence of electron irregularities at the Bragg scale. In section 2 we thus briefly review the main results of the *Cho et al.* [1992] theory and discuss currently available supporting and contradicting evidence. The conclusion of this assessment is that the main physical idea, i.e., the electron diffusion reduction due to ambipolar forces between electrons and charged aerosols, is indeed correct. However, the detailed quantitative understanding of the involved quantities, in particular the threshold ratio between the aerosol charge and the free electron number density, $N_A|Z_A|/n_e$, needed for the electron diffusion reduction, turns out to be poor and deserves closer inspection. In section 3 we then present a detailed case study of in situ measurements of electrons and simultaneous and common volume ground based observations of PMSE and NLCs. Motivated by these observations we propose that the existence of PMSE is rather a function of $N_A|Z_A|r_A^2$ than of $N_A|Z_A|$ and we use a microphysical model to show that $N_A|Z_A|r_A^2$ closely reproduces the main features of our observations. In section 4 we further corroborate this "proxy" for PMSE by comparing proxy properties to the mean altitude range, mean altitude of maximum PMSE signal, and the altitude distribution of the maximum PMSE signal. In section 5, we finally discuss the proxy in the light of currently available theories for PMSE in the VHF band.

2. The *Cho et al.* [1992] Theory Reviewed

2.1. Main Results

[6] The investigation by *Cho et al.* [1992] describes the physical link between electron biteouts observed with rocket-borne sensors [*Ulwick et al.*, 1988] and the phenomenon that electron irregularities exist at scales as small as the Bragg scale of a VHF radar though they should be immediately dissipated by molecular diffusion. The main points of the theory are depicted in Figure 1. In a biteout situation, small aerosol particles of large number density N_A (typical number densities $\sim$1000/cm^{-3}, typical radii $\sim$10 nm) capture on average one electron from the gas phase. Thus they acquire a total charge number density of $N_A|Z_A|$, where $Z_A = -1$ is the charge number of a single particle. As a consequence the remaining free electron number density n_e is depleted in the altitude range with aerosol particles. I.e.,

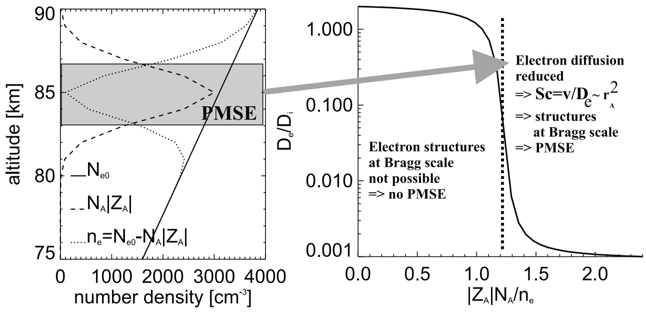

Figure 1. Left panel: Schematic picture of typical altitude profiles of electrons and charged aerosol particles in a "biteout" situation. The shaded area indicates the altitude region where according to *Cho et al.* [1992] PMSE can occur. Right panel: Schematic presentation of Figure 1 by *Cho et al.* [1992] (copyright by the American Geophysical Union): Electron diffusion coefficient D_e in units of the positive ion diffusion coefficient D_i as a function of the charge bound to the aerosol particles, $|Z_A|N_A$, compared to the free electron number density n_e.

in the simplest case that $N_{e0} \gg N_A$, $n_e = N_{e0} - N_A|Z_A|$, where N_{e0} is the undisturbed electron number density in the absence of particles (see left panel of Figure 1). If the depletion is considerably large it is commonly termed a "biteout". For more details about the explanation of electron biteouts including a general discussion of the charge balance in the presence of aerosol particles, see the papers by *Reid* [1990], *Jensen and Thomas* [1991], and *Rapp and Lübken* [2001].

[7] Based on the diffusion theory of *Hill* [1978], *Cho et al.* [1992] constructed a simple model which describes the electron diffusion in a plasma consisting of electrons, one species of positive ions and one species of charged aerosol particles. The main result of this model investigation is shown in the right hand panel of Figure 1: aerosol charge number densities small compared to the free electron number density only lead to minor departures of the electron diffusion coefficient from the ambipolar result ($D_e = 2D_i$; D_i: diffusion coefficient of positive ions). However, if $N_A|Z_A|/n_e$ becomes larger than $\sim$1.2 (as expected in a biteout situation), D_e is drastically reduced and asymptotically reaches the value of the aerosol diffusion coefficient, i.e., $D_e \approx D_A = 0.43D_i/r_A^2$ where r_A is in nm [*Cho et al.*, 1992]. For example, the presence of particles with a radius of 10 nm should lead to a reduction of electron diffusion by a factor of $\sim 2 \times 10^{-3}$ and hence an increase of the decay time of an irregularity by a factor of $\sim$500. The physical explanation for this result is as follows: For $N_A|Z_A|/n_e > 1.2$ negatively charged aerosol particles dominate the plasma charge balance. This means that irregularities in the aerosol charge number density lead to anti-correlated irregularities in the electron gas due to Coulomb repulsion. Then, the electron irregularities can only decay with the decay time of the irregularities in the aerosol particles. Hence, electron irregularities at the Bragg scale can prevail once they have been created and lead to enhanced radar scattering.

[8] Note that the entire mechanism outlined above also works in the case of positively charged particles and associated electron enhancements. Then the threshold of $N_A|Z_A|/n_e$ is moderately decreased to a value of 0.6. How-

ever, since the experimental evidence for positively charged aerosols is very scarce (i.e., only one rocket flight) [*Havnes et al.*, 1996b] and the physical process leading to this positive charge is not well understood [*Rapp and Lübken*, 1999] we restrict our current discussion to the case of negatively charged particles and accompanying electron biteouts.

2.2. Supporting Evidence

[9] What kind of experimental evidence supports the idea of electron diffusion reduction due to negatively charged aerosol particles?

1. The first and most important point is that electron biteouts or at least electron depletions have frequently been found in at least part of the altitude range with PMSEs [e.g., *Ulwick et al.*, 1988; *Lübken and Rapp*, 2001]. Furthermore, *Rapp et al.* [2002a] pointed out that in the majority of available observations $N_A|Z_A|/n_e$ was larger than 1 at least at altitudes with the largest depletion of electron densities (their Tables 2 and 3).

2. Note, furthermore, that the described mechanism requires the existence of the small-scale irregularities not only in the electrons but certainly also in the aerosol particles: As described in section 2.1. it is the Coulomb repulsion between the two negatively charged species which "binds" the disturbance in the electrons to an opposite disturbance of slowly diffusing aerosol particles. Hence, an anticorrelation between electron and aerosol particle fluctuations is expected. In fact, *Havnes et al.* [1996a] have measured such meter scale irregularities in aerosol charge number density together with the expected anti-correlated electron fluctuations. More recently, also *Mitchell et al.* [2001] have reported similar results.

3. A reduced electron diffusion coefficient corresponds to a large Schmidt number Sc = ν/D_e where ν is the kinematic viscosity. In the absence of charged aerosol particles Sc is expected to be close to 1. However, in situ observations of the fine scale structure of neutrals and electrons in PMSEs have yielded Sc numbers considerably larger than $\sim$1 [*Lübken et al.*, 1994]. In addition, *Lübken et al.* [1998] determined identical Schmidt numbers from two completely independent methods: both the analysis of small-scale measurements of neutrals and electrons and the combination of charged aerosol particle measurements with a microphysical model of electron charging yielded values of Sc $\approx$ 400.

4. Additional independent evidence came from a recent radar experiment where the EISCAT VHF radar detected PMSE in a volume where the electron gas was periodically heated to a temperature of $\sim$3000 K [*Chilson et al.*, 2000; *Belova et al.*, 2001]. During the periods where the electron gas was heated the PMSE disappeared with a time constant of less than $\sim$1 s and also reappeared immediately when the heater was switched off. This observation was interpreted by *Rapp and Lübken* [2000] who modeled this situation by considering the electron temperature dependence of the electron diffusivity reduction due to charged aerosol particles. Thus *Rapp and Lübken* [2000] could both explain the fast fade out of the PMSE as well as the instantaneous recovery.

5. Finally, *Rapp et al.* [2002a] reported observations showing a significant anticorrelation between large electron number densities and PMSE power during a strong solar proton event. *Rapp et al.* [2002a] interpreted this observation with the idea that $N_A|Z_A|/n_e$ should decrease due to an increasing n_e when $N_A|Z_A|$ remains approximately constant (as expected from current aerosol charging models).

2.3. Contradicting Evidence

[10] Though the supporting evidence for the electron diffusion reduction mechanism is strong we nevertheless need to stress that there is also evidence which at least partly contradicts *Cho et al.*'s [1992] results:

1. The strongest contradicting evidence comes from in situ observations of both electron densities and charged particles in PMSEs, which showed that at least in part of the PMSE altitude range the criterion $N_A|Z_A|/n_e > 1.2$ was not fulfilled. For example, *Croskey et al.* [2001] presented electron measurements in the vicinity of PMSEs which clearly showed that the PMSEs existed at altitudes where a depletion of electrons was merely detectable. Similar features were also observed by *Blix* [1999] and *Havnes et al.* [2001] and are systematically discussed in the paper by *Blix et al.* [2003].

2. Furthermore, *Rapp et al.* [2002a] noted that the observed anticorrelation between PMSE power and electron number densities during a solar proton event only started at very large electron number densities of $\sim 10^5/\mathrm{cm}^3$. They concluded that based on current knowledge about the expected number densities of aerosol particles the observations were inconsistent with the PMSE criterion $N_A|Z_A|/n_e > 1.2$ and emphasized that the role of charged aerosols in the creation of PMSE is not yet completely understood.

[11] In summary of section 2, we conclude that there are several independent experimental indications that the reduction of electron diffusion due to the presence of charged aerosol particles is the key physical process allowing for the presence of PMSE. On the other hand, different observations show that the condition for this diffusion reduction to take place is not completely understood and needs further investigations to be identified. In the next section we proceed and present observations which to our mind are ideally suited to guide us to a better understanding of the role of charged aerosol particles in the creation of PMSE.

3. A Detailed Case Study

3.1. In Situ Observations

[12] On 6 July 1999, 0006:00 UT, the MIDAS sounding rocket (labeled MDMI05) was launched from the island Andøya (69°N) as part of the international MIDAS/DROPPS program into a combined PMSE and (weak) NLC event [*Goldberg et al.*, 2001]. This sounding rocket carried the combined neutral and electron sensor CONE which successfully measured neutrals and electrons with a typical spatial resolution of $\sim$0.3 m [*Giebeler et al.*, 1993]. In the following we focus on the electron measurements. Results of the neutral air density measurements are given by *Lübken et al.* [2002].

[13] On the ascent part of the rocket trajectory, both the rocket and the ALOMAR Rayleigh/Mie/Raman lidar per-

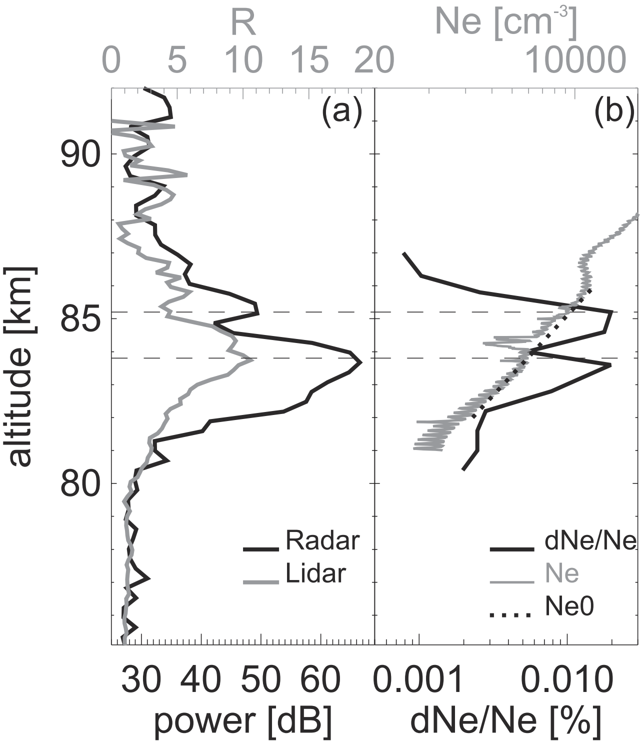

Figure 2. Panel a: Echo power observed with the ALOMAR VHF radar (black line, lower abscissa) averaged from 0:08–0:13 UT, 6 July 1999. The thick gray curve shows the backscatter ratio measured with the ALOMAR Rayleigh/Mie/Raman lidar (integration period: 0:08–0:33 UT, upper abscissa). Panel b: Relative electron number density fluctuations at 2.8 m scale observed with the CONE instrument (black curve, lower abscissa). The gray curve indicates the measured electron number density (upper abscissa) whereas the black dotted line represents an estimate of the undisturbed background electron number density.

formed measurements in the atmospheric volume probed by the ALOMAR VHF radar (frequency = 53.5 MHz, Bragg scale = 2.8 m) [*Latteck et al.*, 1999; *von Zahn et al.*, 2000]. In the left panel of Figure 2 we present the observed radar echo power which reveals a PMSE double structure with the primary peak at 83.7 km and a weaker secondary peak at 85.2 km. The ALOMAR Rayleigh/Mie/Raman lidar measured a weak but significant NLC (lidar backscatter ratio $R \sim 10$) which coincided with the lower PMSE maximum. From our small-scale electron number density measurements we have determined the relative electron number density fluctuations at 2.8 m scale. This quantity is easily derived from the power spectrum of a time series of the measured fluctuations making use of the relation $\Delta n_e/n_e$ (l = 2.8 m) = $100\sqrt{2\ PSD(l = 2.8\,\mathrm{m})}$, where $\Delta n_e/n_e$ (l = 2.8 m) are the electron number density fluctuations (in percent) and PSD(l = 2.8 m) is the power spectral density at the Bragg scale, respectively [*Blix et al.*, 2003].

[14] Just like the radar echo the electron fluctuations show a significant double peak structure (Figure 2, panel b) though it must be noted that there is a slight altitude shift between the radar echoes and the electron fluctuations. Furthermore, the electron fluctuations do not show the difference in signal strength between the two maxima which is observed by the radar. However, it must be kept in mind that the radar echoes are received from an atmospheric volume of roughly 10 km in diameter and a thickness of 300 m whereas the rocket only yields "point"-measurements. Moreover, the radar data have been averaged over 5 min in order to yield a reasonable statistical significance of the observed structures, while the rocket measurements have been obtained during less than 10 s. Taking these arguments into account we do not consider the differences between the radar and the rocket results significant. Our in situ measurements demonstrate that the radar waves are indeed scattered by electron fluctuations at the Bragg scale in agreement with standard radar theory [e.g., *Woodman and Guillen*, 1974]. Unlike during previous measurements [e.g., *Ulwick et al.*, 1988] we recognize that the absolute electron number density does not show a biteout throughout the altitude range with strong electron fluctuations. In fact, only at altitudes between 84 and 85 km the electron number density is markedly depleted whereas at the lower PMSE peak the electron profile is smooth and undisturbed (except for the modulation due to the rocket spin). This implies that for the lower part of the PMSE one of the standard assumptions

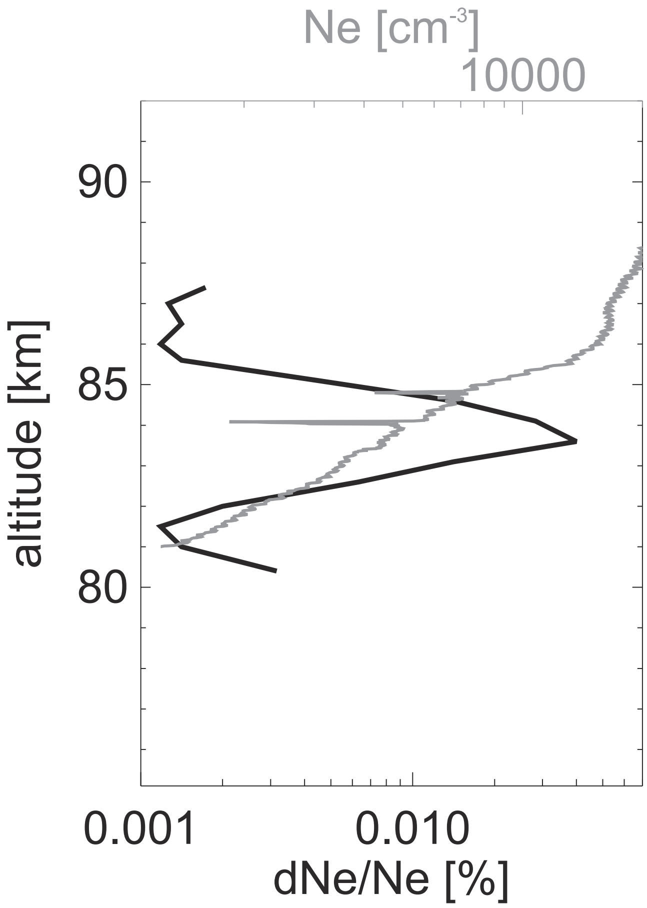

Figure 3. Relative electron number density fluctuations at 2.8 m scale (black line, lower abscissa) together with absolute electron number densities measured on the down-leg part of the rocket trajectory (gray line, upper abscissa).

for the existence of PMSE, i.e., $|Z_A|N_A/n_e > 1.2$, is not fulfilled, though strong fluctuations are observed (see also section 2.3). As shown in Figure 3 the situation is similar during the descent part of the rocket trajectory. Again, the electron number density shows significant depletions only in a small part of the altitude range where significant fluctuations at 2.8 m scale (and thus PMSE) are observed. In fact, the biteouts even appear as single sharp layers with an extent of only ~100 m whereas the altitude range with strong fluctuations extends over several kilometers, i.e., from ~81.5 to 86 km. Note, that, even though very narrow, the biteouts are well resolved by the CONE electron probe which has an altitude resolution of less than 0.3 m (see *Blix et al.* [2003] for more details concerning the experimental technique and related uncertainties).

3.2. Discussion of Experimental Results; The Proxy

[15] In the previous section we have presented PMSE observations and electron measurements revealing an electron biteout in only a small part of the entire PMSE altitude range. The observations presented in Figures 2 and 3 are thus not consistent with *Cho et al.*'s [1992] theory which requires $N_A|Z_A|/n_e \geq 1.2$ (and thus a biteout) in the whole PMSE altitude range.

[16] In this section we propose a new "proxy" for the existence of PMSE. The motivation for introducing this proxy is twofold: the main motivation is to establish an empirically motivated relation between aerosol properties and PMSE which can guide us to find a more complete theory. Second, it is our aim to find an easy parametrization for PMSE which can be used in complicated 3-D circulation models which also treat mesospheric ice particles like the one of *Berger and von Zahn* [2002]. With a suitable parametrization for PMSE these models would be perfect tools for studying, e.g., tidal signatures or the long debated difference between Northern and Southern hemisphere PMSEs [*Balsley et al.*, 1993, 1995].

[17] As explained in section 2 the existence of small-scale irregularities requires the reduction of electron diffusion in order to maintain structures at the radar half wavelength. Similar to the ideas by *Havnes et al.* [2001], we propose that PMSE reflectivity η should be proportional to $|Z_A|N_A$, i.e., the charge number density of aerosol particles. We note that this relation can, however, only be valid in cases where there are enough free electrons left for the scattering of the VHF waves. In fact, observations presented by *Blix et al.* [2003] show that on some rare occasions an anticorrelation between $|Z_A|N_A$ and PMSE reflectivity is observed because the background electron number density is too drastically diminished by the ice particles. In the present study, however, we only consider cases where such an extreme situation does not exist.

[18] Apart from the proportionality to $|Z_A|N_A$, the observations presented in section 3.1 clearly show that there must be other contributions as well: Otherwise we should not observe PMSEs (or electron fluctuations) at altitudes where the electron profile does not reveal a biteout. We find it particularly intriguing that in the left panel of Figure 2 our common volume radar and lidar measurements show that the lowermost PMSE peak coincides with an NLC indicative of a few but large and thus visibly observable ice particles. Since the reduction of electron diffusivity by charged aerosols varies like r_A^2 [*Cho et al.*, 1992] (see section 2), we thus propose that η is also proportional to r_A^2, i.e.,

$$\eta \propto \underbrace{|Z_A|N_A r_A^2}_{P} \tag{1}$$

Formulating this proxy we thus propose that the reduced electron diffusivity due to the large and heavy charged aerosol particles is the most important and necessary condition for PMSE which can account for the majority of observed features. This reduction can, however, not only be achieved by the presence of many charged aerosols (i.e., $N_A|Z_A|/n_e > 1.2$) as proposed by *Cho et al.* [1992] but also by the presence of a few but large particles (i.e., small $N_A|Z_A|$ compensated by large r_A).

[19] In order to show that P is consistent with our observations we now apply a microphysical model of the generation and growth of charged ice particles in the polar summer mesopause region.

3.3. Microphysical Model Simulations

[20] In order to simulate the microphysical processes of ice particle formation in the polar summer mesopause environment we apply the Community Aerosol and Radiation Model for Atmospheres (CARMA) model which is an extension of former NLC models by *Turco et al.* [1982] and *Jensen et al.* [1989]. A recent application of CARMA to the problem of the interaction between gravity waves and noctilucent clouds has been presented by *Rapp et al.* [2002b]. The CARMA model treats three completely interactive constituents: meteoric smoke particles, water vapor, and ice particles. The height profile and the size distribution of meteoric smoke particles is calculated as described by *Hunten et al.* [1980] and the background water vapor is initialized according to the model results by *Körner and Sonnemann* [2001]. As for the ice particles, microphysical processes like nucleation and condensational growth are treated as well as particle sedimentation and transport. In order to model the situation shown in Figure 2 as realistically as possible we further use a temperature profile measured shortly after the measurements of the rocket payload MDMI05 with the falling sphere technique [e.g., *Schmidlin*, 1991]. Unfortunately, we were not able to derive a temperature profile from the CONE instrument since the absolute neutral air density measurement with CONE was hampered by a large coning motion of the rocket payload avoiding the correction of aerodynamical effects (see *Rapp et al.* [2001] for more details on this technique).

[21] To derive charged ice particle number densities and profiles of P we have combined the CARMA model with the ice particle charging model described by *Rapp and Lübken* [2001]. With this model, aerosol charges are calculated by balancing diffusion fluxes of electrons and positive ions toward the aerosol particles. This balancing yields 1 negative elementary charge for particles smaller than 10 nm and a linearly increasing charge number for particles with larger radii (up to five negative elementary charges for r_A = 100 nm). Since the CARMA model yields a particles size distribution rather than one particular particle size and

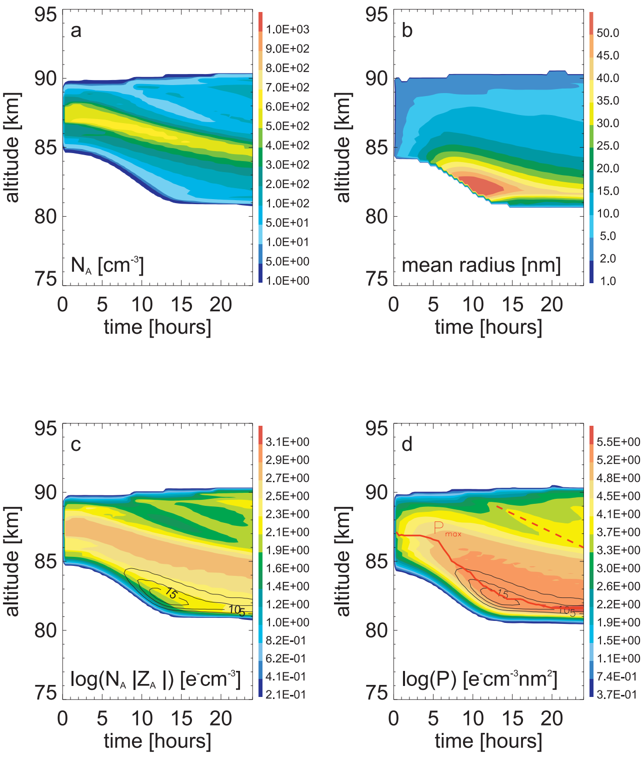

Figure 4. Panel a: Colored contours of the ice number density calculated with the CARMA model for 24 hours of simulation time. Panel b: Mean ice radii calculated with CARMA. Panel c: Colored contours of the logarithm of the ice charge number density calculated with a combination from CARMA results with an aerosol charging model. The black isolines indicate a lidar backscatter ratio which would be observed by a lidar operating at 532 nm. Panel d: Same as Panel c but for proxy values.

number density, the proxy P and the particle charge number density are calculated as follows:

$$N_A|Z_A| = \Sigma_{i=1}^{N} N_{Ai}|Z_{Ai}| \tag{2}$$

$$P = \Sigma_{i=1}^{N} N_{Ai}|Z_{Ai}|r_{Ai}^2 \tag{3}$$

where the summation index i labels the ith size bin of the particle size distribution (see *Rapp et al.* [2002b] for more details on the CARMA model).

[22] In Figure 4 we present model results of ice particle number densities, ice particle radii, ice charge number densities, and proxy values for a time period of 24 hours. Panels 4a and b reveal the picture of the well known growth and sedimentation scenario of mesospheric ice particles. Nucleation takes place between ~84 and 90 km yielding ice particle number densities of up to ~700 cm^{-3}. The particles then settle down and gain size due to further condensation of water vapor onto their surfaces. At the bottom of the ice particle layer the particles reach mean radii between 40 and 50 nm. In Panel 4c we present ice charge number densities. We have also plotted contour lines of the backscatter ratio which a lidar would observe at a wavelength of 532 nm. Lidar backscatter ratios larger than 1 are an indication of an NLC. It is interesting to note that the NLC is located at the lowermost edge of the charged particle layer. However, if the ice charge number density alone were an indication of PMSE our results would imply that the PMSE maximum would be well above the NLC for most of the time (i.e., for t > ~6 hours, see Figure 4). Contrary to this, our observations show (Figure 2) that the NLC coincides with a PMSE maximum. We also note that the charge number densities (<1000 e$^-$cm^{-3}) nowhere come close to the electron number densities, e.g., observed during flight MDMI05 (~5000 cm^{-3}). This means that values of $|Z_A|N_A/n_e \geq 1$ are not to be expected based on these calculations. We note however, that the actual ice number densities which determine the ice charge number densities can be significantly enhanced, e.g., due to the passage of the cold phase of internal gravity waves [e.g., *Rapp et al.*, 2002b]. Also, it would be possible to enhance the number of ice particles by enhancing the number of available condensation nuclei which are assumed to follow the altitude- and size-distribution according to *Hunten et al.* [1980] in this work. However, since detailed information on wave parameters or the actual number of condensation nuclei during the period of the described observations is not available we do not speculate further on this point. Rather, we restrict our model simulations to a thermally quiet atmosphere and keep in mind that this assumption might modify our results.

[23] In Panel 4d we finally show the calculated proxy values P. In this figure, we have also marked the altitude of the maximum proxy value with a thick solid red line (labeled $P_{\max}$). Comparing the $P_{\max}$-altitude with the altitude of the maximum simulated lidar backscatter ratio we see that there is an almost perfect agreement between these quantities (after $t \approx 6$ hours). In addition, we have indicated a secondary maximum in the proxy-field with the red dashed line. This secondary maximum is due to a second nucleation cycle of ice particles after ~10 hours of nucleation time (see Panel a) which occurs because of upward transport of water vapor to the mesopause region due to the mean vertical background wind (see the discussion of Figure 8 by *Rapp et al.* [2002b] for more details). In order to provide a more detailed comparison of our model results with the observations presented in Figure 2 we show

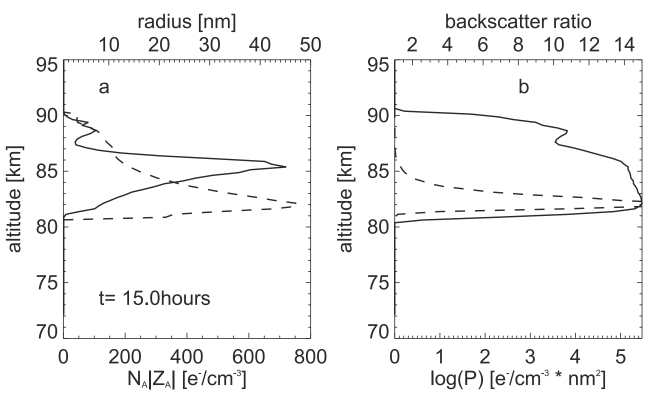

Figure 5. Left panel: Altitude profiles of the aerosol charge density $N_A|Z_A|$ and the aerosol radius. Right panel: Altitude profiles of the proxy P and the lidar backscatter ratio which would be observed at 532 nm wavelength.

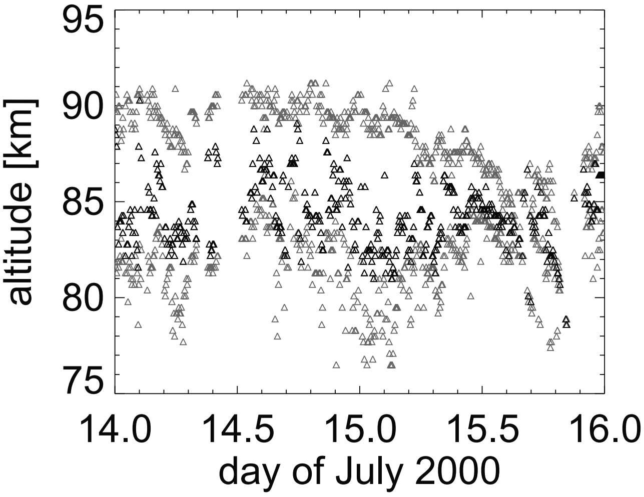

Figure 6. Altitude variation of the upper and lower PMSE edge (gray symbols) as well as of the PMSE maximum (black symbols) during the period from 14 July to 16 July 2000.

altitude profiles of $N_A|Z_A|$, r_A, P, and the lidar backscatter ratio R after 15 hours of model development in Figure 5. There is a very close agreement between our model results and the observations: Both observations and model results show a double layer PMSE (or proxy) with an NLC colocated with the lower PMSE (or proxy) maximum. In addition, we note that just like in the observations the lower maximum is much more pronounced than the upper one and that even the ratio of the signal strengths of the two peaks is comparable for observations and model results: In the observations the ratio between the signal strength of the lower peak at 83.7 km and the upper peak at 85.2 km is 66 dB/50 dB $\approx$ 40. For the model results we find the lower peak at 82 km and the upper peak at 89 km with a signal ratio between the two of $\sim$35. We note that the actual altitudes of the peaks differ between model results and observation, which is, however, not surprising given our model assumption of a constant background temperature profile.

[24] Furthermore, the most pronounced peak in the modeled $N_A|Z_A|$ occurs in between the two maxima of P just like the electron biteout (which according to models is a direct indication of $N_A|Z_A|$) which is located in between the two maxima of the radar signal. Certainly, this peak in $N_A|Z_A|$ does make a significant contribution to the proxy signal, however, the maximum itself is lower down due to the presence of the largest ice particles at the bottom of the layer. Note that this particular feature is not due to our special choice of t = 15 hours: Comparing Panels c and d of Figure 4 it turns out that the maximum aerosol charge density (indicating the most significant disturbance in the electron density profile) is always located in between the two proxy maxima except for the first $\sim$6 hours where the ice particles have not grown large enough in order to let r_A^2 make a significant contribution to P.

[25] In summary, model profiles of $P = N_A|Z_A|r_A^2$ agree well with observations. Thus at least for the discussed case study, P seems to be a reasonable parametrization of PMSE. However, before we can draw definitive conclusions about the validity of our approach we need to find out whether P is consistent with the majority of observations and not only with a single case. In the next section we thus present a comparison of model predictions with mean PMSE properties determined from 3 years of PMSE observations (for the years 1999, 2000, and 2001).

4. Statistical Analysis

[26] Figure 4d contains a further important implication: Due to the strong contribution of r_A^2 to P, the absolute proxy maximum is nearly always located close to the lower edge of the proxy. How does that compare to observations? In Figure 6 we present observational results for an arbitrarily chosen time interval of 2 days in the year 2000. In this example the PMSE maximum is close to the lower edge of the layer in the majority of the presented time interval in agreement with the proxy prediction. We note, however, that natural variability (caused by gravity waves for example) certainly creates a much more dynamical picture than suggested by our model results. In order to investigate whether the situation presented in Figure 6 is typical or not, we have statistically analyzed our PMSE observations (obtained with the ALOMAR VHF-radar) from the core summer months June and July for the years 1999, 2000, and 2001. Individual profiles have been averaged over a period of 5 min. For each averaged profile, we have then determined the altitude of the lower PMSE edge (defined by a signal-to-noise ratio, SNR, of 10 dB), the altitude of maximum PMSE signal strength and the altitude of the upper PMSE edge (SNR = 10 dB). From these altitudes we have then determined the distribution of the quantity d/H (see Figure 7), i.e., the ratio of the distance between the layer maximum and its lower edge and the layer width. The result of this analysis is presented in Figure 8. As can be

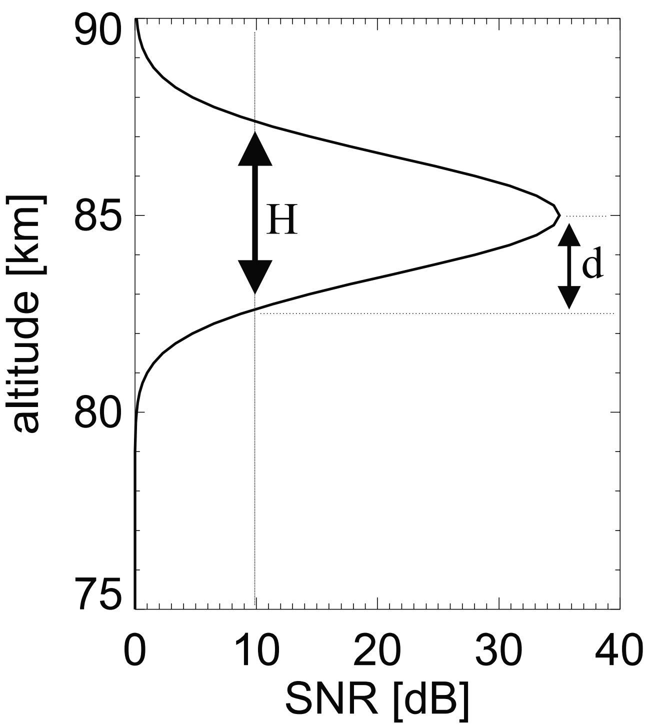

Figure 7. Definition of the PMSE layer width H and distance between the PMSE maximum and its lower edge, d.

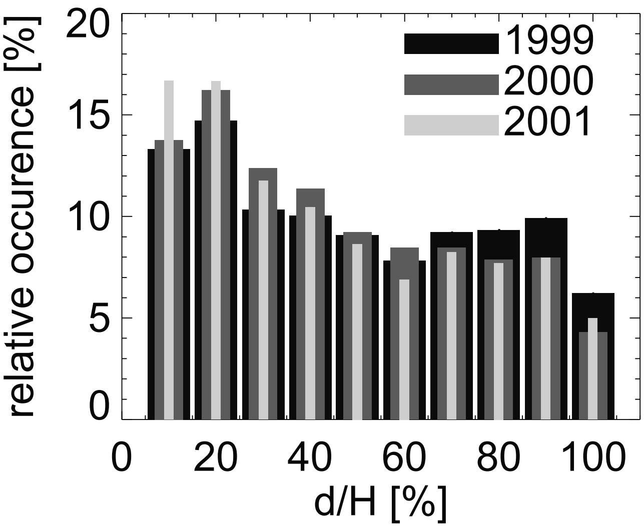

Figure 8. Histogram of the relative occurrence of PMSE with a given relative altitude difference between the maximum PMSE altitude and the lower PMSE edge (defined by a SNR of 10dB) for the PMSE seasons 1999, 2000, and 2001. Note that only PMSE with a width $\geq$ 3 km have been included in this analysis.

seen from Figure 8, the distribution of d/H shows a significant maximum at d/H-values $\leq$30% with peak relative occurrences of $\sim$15% (relative occurrences specified per 10%-interval of d/H). Compared to the occurrences at these low d/H-values it appears that for larger d/H-values the distribution is more or less constant with typical occurrences between 5% and 10%.

[27] We offer the following hypothesis as an explanation for this result: in the absence of large particles (say radii $\leq$35 nm; see Figure 4) the relative altitude distances between the edges of a PMSE layer and the PMSE maximum is mainly a function of the local thermal structure where for example the relatively short presence ($\leq$1 hour) of a local temperature minimum can lead to the formation of many small particles. In this case we would expect that all possible d/H-values occur with the same occurrence rate. However, in cases where particles have had the chance to grow to larger radii (and can be observed as NLC) these large radii make the most significant contribution to the PMSE signal. In this case, the maximum is located in the lower third of the entire PMSE altitude range since the large and heavy particles have already settled down due to gravity.

[28] Note that our current findings do not contradict the results obtained by *von Zahn and Bremer* [1999] who found that in the seasonal average the maximum altitude of PMSEs is $\sim$85 km whereas it is $\sim$83 km for NLC. For their analysis, *von Zahn and Bremer* [1999] did not distinguish between PMSE observations with and without NLC. If this is done, the mean PMSE height in the presence of NLC is $\sim$83–84 km [*Bremer et al.*, 1999] in accordance with our proxy prediction, i.e., that in the presence of large particles (=NLC) the PMSE maximum should occur at the altitude where these large particles occur (=at the NLC height).

[29] Thus the statistics presented in Figure 8 strongly supports the idea that PMSE reflectivity depends on the radius of the particles involved because we do expect the largest ice particles slightly above the bottom of an ice particle layer due to particle growth and sedimentation.

[30] We now compare proxy and PMSE based on time averaged altitude profiles. In Figure 9 we present the mean profile of measured echo powers for the months June and July 2000. In addition, we also show the time average of the proxy field shown in Figure 4. Again, we find that there is an almost perfect agreement between model results for the proxy and PMSE observations: both proxy and PMSE extend from $\sim$80–90 km and peak at $\sim$85 km altitude. The question arises whether this agreement is by chance because of the special atmospheric background situation simulated with CARMA. In order to check the sensitivity of our results for disturbances of the background atmosphere by the transience of, e.g., gravity waves we have also determined mean proxy profiles from CARMA simulations in the presence of gravity waves which recently have been published by *Rapp et al.* [2002b]. With the dashed-dotted (dashed) line we show the mean proxy profile (again averaged over a simulation time of 24 hours) for a simulation with a gravity wave period of $\sim$8 hours (1 hour). Evidently, the action of the waves only lead to minor

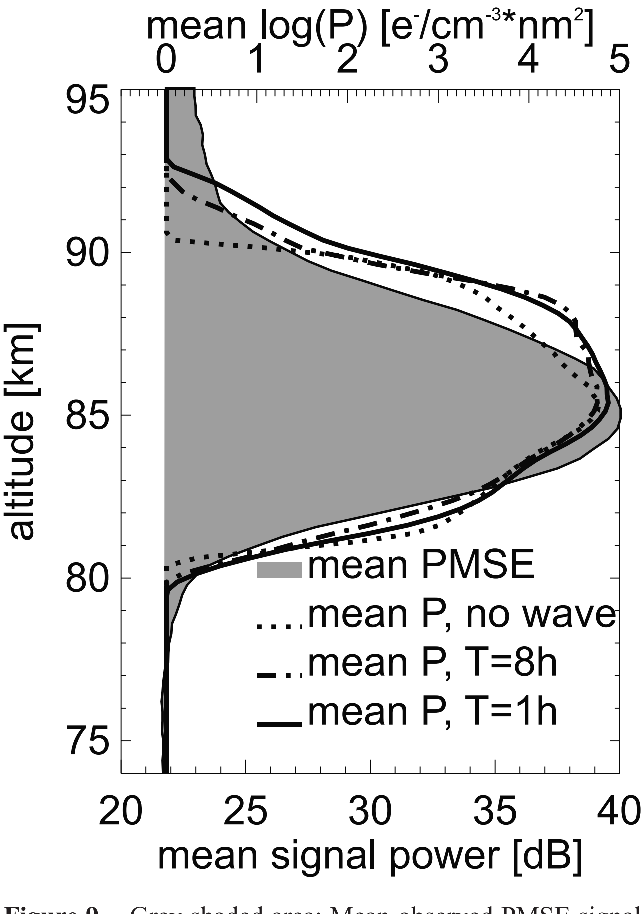

Figure 9. Grey shaded area: Mean observed PMSE signal power during the months June and July 2000. Dotted line: Mean proxy profile obtained by time averaging the results shown in Figure 4d. Solid line and dashed-dotted line: Mean proxy profiles obtained from CARMA simulations including gravity wave activity for wave periods of 8 hours and 1 hour, respectively.

changes as far as the altitude range and the altitude of the maximum mean proxy signal is concerned. Finally, we note that for all simulations, calculated maximum lidar backscatter ratios (which are indicative of NLC altitudes) occur at ~83 km. This value agrees perfectly with the mean NLC centroid height observed at ALOMAR (=83.4 km) during the years 1997–2001 [*Fiedler et al.*, 2003].

5. Discussion: Importance of Other Geophysical Parameters

[31] In order to evaluate the uniqueness of our proxy we now proceed with a discussion of different PMSE theories formulated in the literature. For this we concentrate on the theories for VHF PMSE which leaves the following approaches to our discussion:

1. Dust hole scatter [*Havnes et al.*, 1992]
2. Turbulent scatter with high Schmidt-number [e.g., *Klostermeyer*, 1997]
3. Opalescence [*Trakhtengerts and Demekhov*, 1995]

[32] Among these, we can directly exclude the opalescence theory since it requires very large charge number densities of aerosol particles ($|Z_A| > 1000$) which is in contradiction to all available experimental evidence (and certainly also to our proxy which accounts for PMSE also in the case of small $N_A|Z_A|$ but "large" r_A).

[33] As far as the turbulence approach is concerned we note that only recently *Lübken et al.* [2002] have demonstrated that neutral air turbulence was absent in the majority of the observations investigated. Thus, these authors have suggested that turbulence acts on the preexisting PMSE structures and that it appears likely that there is no direct causally determined connection between turbulence and PMSE.

[34] It thus turns out that apparently the dust-hole scatter theory is the only alternative to our approach. In the following subsection we thus proceed and discuss this theory in detail.

[35] The dust-hole scatter theory was suggested by *Havnes et al.* [1992] and is particularly interesting for the discussion of our observations since it does not necessarily require the existence of many charged aerosol particles dominating the charge balance at PMSE altitudes [see, e.g., *Havnes et al.*, 1992, Figure 9].The main idea is that charged aerosol particles which sediment through a volume filled with vortices in the neutral gas can possibly not penetrate into the center of the vortex. As a consequence, there can be sharp gradients in the aerosol number density at the boundaries of these vortices. Since the aerosol particles are expected to be charged and their charging should leave an equivalent signature in the electron density profile, there should also be a sharp gradient in the electron number density. Then the volume reflectivity can be substantially enhanced compared to the incoherent background scatter. According to *Havnes et al.* [1992], the reflectivity due to one vortex can be expressed as (see Havnes et al.'s equation 36):

$$R^2 \propto \frac{U^2(r_A) r_A^6 F^2(r_A) \rho_A^2}{f_{\mathrm{radar}}^6 K_M^2 R_V^{\frac{8}{3}} \rho_n^2} \tag{4}$$

where $U \propto Z_A/r_A$ is the surface potential of the charged aerosol particle, $F(r) = dN_A(r)/dr$ is the distribution function of the particle sizes, $\rho_{A/n}$ is the mass density of the aerosols/neutrals, f_{radar} the radar frequency, K_M is a scaling factor relating the vortex velocity to a Kolmogorow spectrum, and R_V is the vortex diameter.

[36] For comparison with the proxy we only consider the dependence of R^2 on N_A, Z_A, and r_A and do not speculate about the existence of the vortices themselves which has not yet been experimentally proven. Taking into account the definition of the surface potential U and assuming for simplicity a mono-modal size distribution such that $F(r) = N_A\delta(r - r_A)$ we find that

$$R^2 \propto N_A^2 Z_A^2 r_A^4 \tag{5}$$

[37] It thus turns out that the dust-hole scatter theory yields a dependence of the radar reflectivity which is proportional to the square of our proxy. Just like in our approach it thus suggests a considerable influence of large particles on the radar reflectivity (and also *Havnes et al.* [1992] hinted at the possibility that "the maximum radar reflection [...] could also be low in the dust forming region").

[38] The question is if we can distinguish between the proxy and the dust hole reflectivity based on available observations. In general, this is a difficult task since for both approaches the volume reflectivity should not only depend on the aerosol charge density but also on the aerosol radius. Until now, only a couple of successful sounding rocket measurements have been performed where charge number densities of aerosols were measured during a PMSE event [*Havnes et al.*, 1996b, 2001; *Mitchell et al.*, 2001; *Croskey et al.*, 2001]. Unfortunately, none of these observations yielded experimental facts about the radii of the aerosol particles. It thus turns out that a direct comparison of $N_A|Z_A|r_A^2$ and $N_A^2|Z_A|^2r_A^4$ with the observed radar signal cannot be performed.

[39] However, if the aerosol radius stays approximately constant over the observed altitude range then we should expect a one to one correspondence between $N_A|Z_A|$ and the radar SNR. In order to distinguish between the dust-hole scatter theory and our approach it thus appears to be a good strategy to search for observations where we can assume that the aerosol radius did not vary significantly over the altitude range with PMSE. Provided that this condition is fulfilled we can then test if measured radar signals are proportional to $N_A|Z_A|$ (as proposed in this paper) or to $N_A^2|Z_A|^2$ (as proposed by *Havnes et al.* [1992]).

[40] *Mitchell et al.* [2001] and *Croskey et al.* [2001] show results (obtained 30 min before our measurements) which are qualitatively similar to our observations (i.e., signatures of charged aerosol particles and an electron biteout in the upper part of the PMSE and an NLC in the lower part, see Figure 4 of *Croskey et al.* [2001] and thus also imply a significant variation of the aerosol radius over the altitude range with PMSE. Contrary to this, *Havnes et al.* [1996] and *Havnes et al.* [2001] have reported results from two rocket soundings where the measured aerosol charge densities resembled the structure of simultaneously observed PMSE very closely. Furthermore, during both flights ground based lidars confirmed the absence of NLC [*Lübken et al.*, 1996; *Goldberg et al.*, 2001]. For these flights, it thus seems

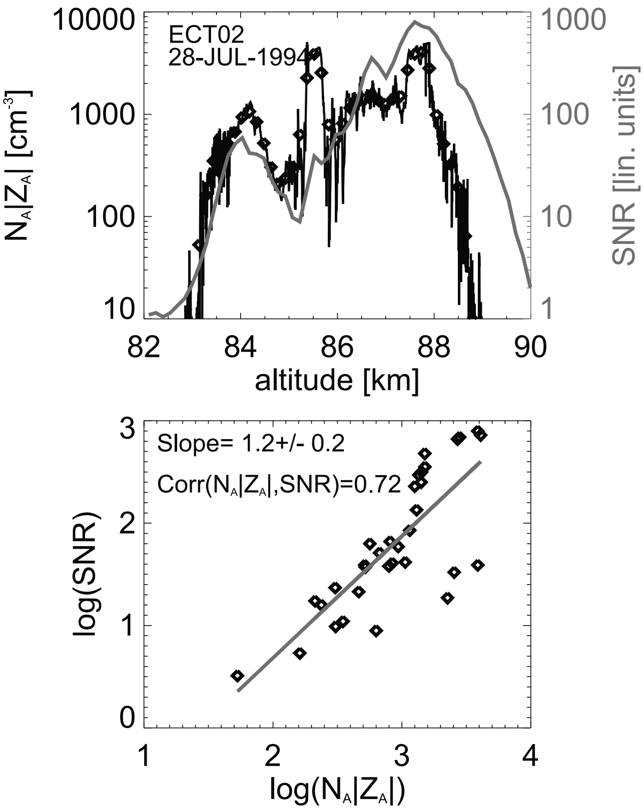

Figure 10. Upper panel: Measured aerosol charge number density (black line, left abscissa) as a function of altitude during sounding rocket flight ECT02 [*Havnes et al.*, 1996b]. The gray line (right abscissa) shows the measured radar SNR profile in linear units. Lower panel: Logarithm of SNR as a function of the logarithm of the aerosol charge number density (black symbols). The thick gray line indicates the linear regression to the data yielding a slope of 1.2 ± 0.2.

reasonable to assume that the aerosol radii did not vary significantly with altitude.

[41] Thus, we proceed with an analysis of the relation between $N_A|Z_A|$ and radar SNR measured during the flights ECT02 (28 July 1994) and MDMD06 (6 July 1999) [*Havnes et al.*, 1996b, 2001]. In Figure 10 we present a comparison of the measured aerosol charge density and the radar signal-to-noise ratio (SNR) for flight ECT02. In the lower panel of this figure we show a scatterplot of the logarithms of the radar SNR versus the aerosol charge number density $N_A|Z_A|$. In order to identify the power law between the SNR and $N_A|Z_A|$, i.e., SNR $\propto (N_A|Z_A|)^n$, we have performed a linear regression of these data yielding $n = 1.2 \pm 0.2$. Evidently, the measured data are thus much closer to a slope of 1 than to a slope of 2. (Also note, that the correlation coefficient between the radar SNR and $N_A|Z_A|$ is as large as 0.72 and highly significant: according to Fisher's test the correlation coefficient is well beyond the 99.9% confidence level).

[42] The second case (flight MDMD06) yields less conclusive results: *Havnes et al.* [2001] presented a scatterplot of measured aerosol charge number densities and radar power (see their Figure 2). This scatterplot shows almost no relation between the two quantities for power values <40-45 dB and charge number densities <100/cm^3. If we try to determine the slope of these data for power values >45 dB and $N_A|Z_A| > 100$/cm^3 we obtain a slope of $n = 2.2 \pm 0.6$. The large error of this slope is mainly due to the large scatter of the data and in particular because the $N_A|Z_A|$ measurements only cover a relatively small range between 100/cm^3 and 650/cm^3. In addition, it turns out that the rather large value for n is dominated by only two data points at $N_A|Z_A| \sim 175$/cm^3. If these two points are omitted, we end up with slope values of $n = 1.2 \pm 0.4$, i.e., again much closer to results obtained for flight ECT02.

[43] We thus conclude that the available observations tend to support a dependence of PMSE reflectivity on $(N_A|Z_A|)^n$ with n being closer to 1 than to 2, thus supporting our proxy. However, we are certainly aware of the poor statistics of only two data sets. In order to finally distinguish between the different potential powers of the aerosol charge density in determining the radar volume reflectivity, more observational data (at best with the simultaneous measurement of aerosol radii) are needed.

6. Summary and Conclusion

[44] We have presented experimental evidence from a rocket flight and simultaneous and common volume ground based radar and lidar observations that a commonly assumed condition for the existence of PMSE was not fulfilled [*Cho et al.*, 1992; *Cho and Röttger*, 1997]: only in a small part of the entire altitude range with PMSE the rocket-borne electron sensor CONE detected a significant electron biteout, indicative of a large number of charged aerosol particles such that $N_A|Z_A|/n_e \geq 1.2$. Nevertheless, the spectral analysis of the small-scale electron fluctuations showed that the observed PMSE was well correlated with fluctuations at the radar Bragg scale (2.8 m). Thus small-scale electron fluctuations existed at altitudes where a large scale (altitude range of PMSE: several kilometers) biteout did not exist. Furthermore, we found that the lowermost peak of the PMSE coincided with an NLC.

[45] We thus take these observational results as strong evidence that it is not $N_A|Z_A|$ alone which is decisive if PMSE can exist or not, but the product $N_A|Z_A|r_A^2$. Furthermore, we propose that $N_A|Z_A|r_A^2$ can be used as a microphysical proxy for PMSE. In order to investigate the feasibility of this approach we used a microphysical model of ice particle growth in the polar summer mesopause region in combination with a model of aerosol charging. We calculated altitude profiles of ice particle number densities, radii, charge number densities, proxy values, and lidar backscatter ratios yielding features very similar to the observations. For example, after a simulation time of 15 hours the proxy showed two local maxima with the lowermost maximum located at the same altitude as the maximum lidar backscatter ratio and the maximum ice charge number density located in between the two proxy maxima. In this scenario, a double layer PMSE (or proxy) is explained by the layering of two ice particle layers above each other.

[46] In addition, the model results showed that in the majority of cases the maximum proxy signal is close to the lower proxy edge. In fact, PMSEs observed at Andøya show

a distribution of relative distances between the maximum PMSE signal and the lower PMSE edge which has a significant peak in the distribution for relative distances of $\leq$30%. Having in mind that the largest ice particles are expected at the lower edge of the ice particle layer due to sedimentation we consider this finding as a strong support for our suggestion that the radar echo is proportional to r_A^2. Finally, the proxy does a good job in reproducing the mean altitude range of PMSE as well as its mean peak signal altitude.

[47] We have compared our proxy to currently available theories for PMSE in the VHF band and found that the proxy is consistent with available observations whereas these theories are not. Nevertheless, it is obvious that more observations like the ones by *Havnes et al.* [1996b, 2001] are needed.

[48] At the current stage, we conclude that $|Z_A|N_A r_A^2$ gives a good description of several relevant properties of PMSE and it thus appears likely that the actual scattering mechanism leading to PMSE is also physically linked to that proxy. We are aware that our results do not provide a theory of PMSE reflectivity, however, we consider it an important constraint on the way to a complete understanding of the microphysical processes leading to PMSE. Furthermore, the proxy provides a simple parametrization for PMSE which can be used in complicated 3-D models dealing with ice particles in the mesopause region.

[49] **Acknowledgments.** The MIDAS project was supported under DLR-grant 50 OE 9802 and grant 115980/431 from the Norwegian Research Council. We appreciate the excellent work of the members of the DLR Mobile Raketenbasis and the staff of the Andøya Rocket Range.

References

Balsley, B. B., R. F. Woodman, M. Sarango, J. Urbina, R. Rodriguez, E. Ragaini, and J. Carey, Southern-hemisphere PMSE: Where are they?, *Geophys. Res. Lett.*, *20*, 1983–1985, 1993.

Balsley, B. B., R. F. Woodman, M. Sarango, R. Rodriguez, J. Urbina, E. Ragaini, J. Carey, M. Huaman, and A. Giraldez, On the lack of southern-hemisphere PMSE, *J. Geophys. Res.*, *100*, 11,685–11,693, 1995.

Belova, E., P. Chilson, M. Rapp, and S. Kirkwood, Electron temperature dependence of PMSE power: Experimental and modelling results, *Adv. Space Res.*, *28*(7), 1077–1082, 2001.

Berger, U., and U. von Zahn, Icy particles in the summer mesopause region: 3-d modelling of their environment and 2-d modelling of their transport, *J. Geophys. Res.*, *107*(A11), 1315, doi:10.1029/2001JA000316, 2002.

Blix, T. A., Small scale plasma and charged aerosol variations and their importance for polar mesosphere summer echoes, *Adv. Space Res.*, *24*, 537–546, 1999.

Blix, T. A., M. Rapp, and F.-J. Lübken, Relations between small-scale electron number density fluctuations, radar backscatter, and charged aerosol particles, *J. Geophys. Res.*, *108*, doi:10.1029/2002JD002430, in press, 2003.

Bremer, J., G. von Cossart, P. Hoffmann, W. Singer, and J. Röttger, Simultaneous and common volume PMSE and NLC observations in northern Europe, paper presented at the XXVI URSI General Assembly, Toronto, Canada, August 13–21, 1999.

Chilson, P. B., E. Belova, M. Rietveld, S. Kirkwood, and U.-P. Hoppe, First artificially induced modulation of PMSE using the EISCAT heating facility, *Geophys. Res. Lett.*, *27*, 3801–3804, 2000.

Cho, J. Y. N., and J. Röttger, An updated review of polar mesosphere summer echoes: Observation, theory, and their relationship to noctilucent clouds and subvisible aerosols, *J. Geophys. Res.*, *102*, 2001–2020, 1997.

Cho, J. Y. N., T. M. Hall, and M. C. Kelley, On the role of charged aerosols in polar mesosphere summer echoes, *J. Geophys. Res.*, *97*, 875–886, 1992.

Croskey, C., J. Mitchell, M. Friedrich, K. Torkar, U.-P. Hoppe, and R. Goldberg, Electrical structure of PMSE and NLC regions during the DROPPS program, *Geophys. Res. Lett.*, *28*, 1427–1430, 2001.

Czechowsky, P., R. Rüster, and G. Schmidt, Variations of mesospheric structures in different seasons, *Geophys. Res. Lett.*, *6*, 459–462, 1979.

Ecklund, W. L., and B. B. Balsley, Long-term observations of the arctic mesosphere with the MST radar at Poker Flat, Alaska, *J. Geophys. Res.*, *86*, 7775–7780, 1981.

Fiedler, J., G. Baumgarten, and G. von Cossart, Noctilucent clouds above ALOMAR between 1997 and 2001: Occurrence and properties, *J. Geophys. Res.*, *108*, doi:10.1029/2002JD002419, in press, 2003.

Giebeler, J., F.-J. Lübken, and M. Nägele, CONE - a new sensor for in-situ observations of neutral and plasma density fluctuations, in *Proceedings of the 11th ESA Symposium on European Rocket and Balloon Programmes and Related Research, Montreux, Switzerland (ESA SP), ESA-SP-355*, pp. 311–318, 1993.

Goldberg, R., et al., Dropps: A study of the polar summer mesosphere with rocket, radar and lidar, *Geophys. Res. Lett.*, *28*, 1407–1410, 2001.

Havnes, O., F. Melandsø, C. L. Hoz, T. K. Aslaksen, and T. Hartquist, Charged dust in the Earth's mesopause: Effects on radar backscatter, *Phys. Scr.*, *45*, 535–544, 1992.

Havnes, O., L. I. Næsheim, T. Hartquist, G. E. Morfill, F. Melandsø, B. Schleicher, J. Trøim, T. Blix, and E. Thrane, Meter-scale variations of the charge carried by mesospheric dust, *Planet. Space Sci.*, *44*, 1191–1194, 1996a.

Havnes, O., J. Trøim, T. Blix, W. Mortensen, L. I. Næsheim, E. Thrane, and T. Tønnesen, First detection of charged dust particles in the Earth's mesosphere, *J. Geophys. Res.*, *101*, 10,839–10,847, 1996b.

Havnes, O., A. Brattli, T. Aslaksen, W. Singer, R. Latteck, T. Blix, E. Thrane, and J. Trøm, First common volume observations of layered plasma structures and polar mesospheric summer echoes by rocket and radar, *Geophys. Res. Lett.*, *28*, 1419–1422, 2001.

Hill, R. J., Nonneutral and quasi-neutral diffusion of weakly ionized multiconstituent plasma, *J. Geophys. Res.*, *83*, 989–998, 1978.

Hill, R. J., D. E. Gibson-Wilde, J. A. Werne, and D. C. Fritts, Turbulence-induced fluctuations in ionization and application to PMSE, *Earth, Planets Space*, *51*, 499–513, 1999.

Hunten, D. M., R. P. Turco, and O. B. Toon, Smoke and dust particles of meteoric origin in the mesosphere and stratosphere, *J. Atmos. Sci.*, *37*, 1342–1357, 1980.

Jensen, E., and G. E. Thomas, Charging of mesospheric particles: Implications for electron density and particle coagulation, *J. Geophys. Res.*, *96*, 18,603–18,615, 1991.

Jensen, E., G. E. Thomas, and O. B. Toon, On the diurnal variation of noctilucent clouds, *J. Geophys. Res.*, *94*, 14,693–14,702, 1989.

Kelley, M. C., D. T. Farley, and J. Röttger, The effect of cluster ions on anomalous VHF backscatter from the summer polar mesosphere, *Geophys. Res. Lett.*, *14*, 1031–1034, 1987.

Klostermeyer, J., A height- and time-dependent model of polar mesosphere summer echoes, *J. Geophys. Res.*, *102*, 6715–6727, 1997.

Körner, U., and G. Sonnemann, Global 3d-modelling of the water vapor concentration of the mesosphere/mesopause region and implications with respect to the NLC region, *J. Geophys. Res.*, *106*, 9639–9651, 2001.

Latteck, R., W. Singer, and H. Bardey, The ALWIN MST radar: Technical design and performance, in *Proceedings of the 14th ESA Symposium on European Rocket and Balloon Programmes and Related Research, Potsdam, Germany (ESA SP-437), ESA-SP-437*, pp. 179–184, 1999.

Lübken, F.-J., Seasonal variation of turbulent energy dissipation rates at high latitudes as determined by in situ measurements of neutral density fluctuations, *J. Geophys. Res.*, *104*, 13,441–13,456, 1997.

Lübken, F.-J., and M. Rapp, Modelling of particle charging in the polar summer mesosphere, part 2, Application to measurements, *J. Atmos. Sol.-Terr. Phys.*, *63*, 771–780, 2001.

Lübken, F.-J., G. Lehmacher, T. Blix, U.-P. Hoppe, E. Thrane, J. Cho, and W. Swartz, First in-situ observations of neutral and plasma density fluctuations within a PMSE layer, *Geophys. Res. Lett.*, *20*, 2311–2314, 1993.

Lübken, F.-J., J. Giebeler, T. Blix, E. Thrane, W. Singer, and J. Bremer, In-situ measurement of the Schmidt number within a PMSE layer, *Geophys. Res. Lett.*, *21*, 1651–1654, 1994.

Lübken, F.-J., K.-H. Fricke, and M. Langer, Noctilucent clouds and the thermal structure near the Arctic mesopause, *J. Geophys. Res.*, *101*, 9489–9508, 1996.

Lübken, F.-J., M. Rapp, T. Blix, and E. Thrane, Microphysical and turbulent measurements of the Schmidt number in the vicinity of polar mesosphere summer echoes, *Geophys. Res. Lett.*, *25*, 893–896, 1998.

Lübken, F.-J., M. Rapp, and P. Hoffmann, Neutral air turbulence and temperatures in the vicinity of polar mesosphere summer echoes, *J. Geophys. Res.*, *107*(D15), 4273, doi:10.1029/2001JD000915, 2002.

Mitchell, J., C. Croskey, and R. Goldberg, Evidence for charged aerosol particles and associated meter-scale structure in identified PMSE/NLC regions, *Geophys. Res. Lett.*, *28*, 1423–1426, 2001.

Rapp, M., and F.-J. Lübken, Modelling of positively charged aerosols in the polar summer mesopause region, *Earth, Planets Space*, *51*, 799–807, 1999.

Rapp, M., and F.-J. Lübken, Electron temperature control of PMSE, *Geophys. Res. Lett.*, *27*, 3285–3288, 2000.

Rapp, M., and F.-J. Lübken, Modelling of particle charging in the polar summer mesosphere, part 1, General results, *J. Atmos. Sol.-Terr. Phys.*, *63*, 759–770, 2001.

Rapp, M., J. Gumbel, and F.-J. Lübken, Absolute density measurements in the middle atmosphere, *Ann. Geophys.*, *19*, 571–580, 2001.

Rapp, M., J. Gumbel, F.-J. Lübken, and R. Latteck, D-region electron number density limits for the existence of polar mesosphere summer echoes, *J. Geophys. Res.*, *107*(D14), 4187, doi:10.1029/2001JD001323, 2002a.

Rapp, M., F.-J. Lübken, A. Müllemann, G. E. Thomas, and E. J. Jensen, Small scale temperature variations in the vicinity of NLC: Experimental and model results, *J. Geophys. Res.*, *107*(D19), 4392, doi:10.1029/2001JD001241, 2002b.

Reid, G. C., Ice particles and electron ‘‘bite-outs’’ at the summer polar mesopause, *J. Geophys. Res.*, *95*, 13,891–13,896, 1990.

Schmidlin, F. J., The inflatable sphere: A technique for the accurate measurement of middle atmosphere temperatures, *J. Geophys. Res.*, *96*, 22,673–22,682, 1991.

Tatarskii, V. I., *The Effects of the Turbulent Atmosphere on Wave Propagation*, Isr. Program for Sci. Transl., Jerusalem, 1971.

Trakhtengerts, V. Y., and A. G. Demekhov, Nonequilibrium electron density fluctuations and wave scattering in the mesosphere, *J. Atmos. Terr. Phys.*, *57*, 1153–1164, 1995.

Turco, R. P., O. B. Toon, R. C. Whitten, R. G. Keesee, and D. Hollenbach, Noctilucent clouds: Simulation studies of their genesis, properties and global influences, *Planet. Space Sci.*, *3*, 1147–1181, 1982.

Ulwick, J. C., K. D. Baker, M. C. Kelley, B. B. Balsley, and W. L. Ecklund, Comparison of simultaneous MST radar and electron density probe measurements during STATE, *J. Geophys. Res.*, *93*, 6989–7000, 1988.

von Zahn, U., and J. Bremer, Simultaneous and common-volume observations of noctilucent clouds and polar mesosphere summer echoes, *Geophys. Res. Lett.*, *26*, 1521–1524, 1999.

von Zahn, U., G. von Cossart, J. Fiedler, K. Fricke, G. Nelke, G. Baumgarten, D. Rees, A. Hauchecorne, and K. Adolfsen, The ALOMAR Rayleigh/Mie/Raman lidar: Objectives, configuration, and performance, *Ann. Geophys.*, *18*, 815–833, 2000.

Woodman, R. F., and A. Guillen, Radar observations of winds and turbulence in the stratosphere and mesosphere, *J. Atmos. Sci.*, *31*, 493–505, 1974.

G. Baumgarten, P. Hoffmann, R. Latteck, F.-J. Lübken, and M. Rapp, Leibniz-Institute of Atmospheric Physics, Schloss-Str. 6, D-18225 Kühlungsborn, Germany. (rapp@iap-kborn.de)

T. A. Blix, Division for Electronics, Norwegian Defence Research Establishment, P.O. Box 25, N-2007 Kjeller, Norway. (Tom-Arild.Blix@ffi.no)